13th International Symposium on Turbulence and Shear Flow Phenomena (TSFP13)
Montreal, Canada, June 25–28, 2024

EXPERIMENTALLY MODELLING DISPERSIVE SCALAR FLUXES IN A 3D PRINTED URBAN ENVIRONMENT USING A WATER TUNNEL

Tomos Rich
Faculty of Engineering and Physical Sciences
University of Southampton
Burgess Road, Southampton SO16 7QF
tjr1u19@soton.ac.uk

Dr Christina Vanderwel
Faculty of Engineering and Physical Sciences
University of Southampton
Burgess Road, Southampton SO16 7QF
C.M.Vanderwel@soton.ac.uk

ABSTRACT

The modelling of urban air pollution requires an understanding of the turbulent processes involved. Measuring these processes requires a high-fidelity experimental study, and this project aims to provide that. An investigation into scalar dispersion over a 3D-printed model of the City of Southampton was carried out. This 1000:1 scale model was created to represent 1 km^2 of Southampton's city centre. Experimentally measuring turbulent scalar fluxes is challenging as it requires both concentration and velocity measurements in the same place, and at the same time. Particle image velocimetry (PIV) and planar laser induced fluorescence (PLIF) were used to measure full fields of these turbulent scalar fluxes. Measurements were carried out in streamwise-vertical and wall-parallel planes to create a detailed map of concentration and velocity data for a case in which a plume from a point source was introduced upstream of this model.

1 Introduction

The risk to public health posed by air pollution is significant (Dziubanek *et al.*, 2017), and living in an urban environment is a risk factor that increases exposure. The world's population is still growing, and is also gravitating more towards these urban environments. This means that a larger proportion of this population will be directly exposed to urban air pollution (United Nations Department of Economic and Social Affairs, 2018). Due to this there is an increasing need for more accurate predictions of urban air pollution.

Both general weather forecasting and the air quality forecasting are dependent on understanding urban air flow and how it transports pollutants. Two of the primary providers of this data within the UK are the Department of Environment, Food, and Rural Affairs (DEFRA) and the Met Office. DEFRA uses a range of modelling techniques to predict air quality, which range from simple ones that can run on a personal computer to advanced models that necessitate the use of a high-performance-computer (HPC)(Williams & Barrowcliffe, 2011). The Met Office produces more of the general weather forecasts within the UK, but also models air quality (Met Office, 2022; Bermous & Steinle, 2015). In order to produce these weather forecasts and predict air quality, the Met Office has exclusive use of a HPC that at the time of its launch in 2016 was ranked within the top 50 most powerful computers in the world (Met Office, 2016). Additionally, London city council has recently introduced new guidance that large new building developments within London must conduct studies on their potential influence on the local urban micro-climate (City of London, 2022). This shows the increasing interest in understanding urban micro-climates and air quality.

Computational models for urban air flow and air pollution detailed above are popular because of their speed and convenience. However, realistic data remains crucial for the development and calibration of the mathematical models required for simulations. Acquiring realistic data for this purpose can only be done through either sensor data in real world scenarios, or through scaled experiments in wind or water tunnels.

2 Literature Review

2.1 Characteristics of urban boundary layers

Urban environments exist within an atmospheric boundary layer. This atmospheric boundary layer varies in depth depending on the roughness of the landscape and is of the order of a kilometer deep. The roughness sublayer of flow over a city extends two to five times the maximum building height. Within this region, modelling the city characteristics becomes extremely difficult as local building geometry makes the flow unpredictable. Above the roughness sublayer, the properties of the atmospheric boundary layer become a function of height and are less sensitive to local geometry.

2.2 Fundamentals of Scalar Transport

The movement of a scalar in a flow is calculated using the scalar transport equation

$$\frac{\partial C}{\partial t} + U_j \frac{\partial C}{\partial x_j} = \frac{\partial}{\partial x_j}\left(\gamma \frac{\partial C}{\partial x_j} - \overline{cu_j}\right), \tag{1}$$

in which the C term refers to the mean concentration of a flow, and the U_j term refers to the mean flow velocity in the j direction.

In an experimental case with a constant dye release, the first term in this equation ($\frac{\partial C}{\partial t}$) is zero as this term refers to boundary conditions changing in time. The second term ($U_j \frac{\partial C}{\partial x_j}$) is the advective flux of the flow and represents the transport of the scalar by the mean flow. In all cases with a mean flow this is a significant term but that can be fully resolved with only knowledge of the mean conditions.

The third term ($\gamma \frac{\partial C}{\partial x_j}$) is the molecular diffusion term and is assumed to be small for both real urban flows and for experiments carried out in water. The fourth term ($-\overline{cu_j}$) is the turbulent diffusion and this term can be significant but is both difficult to computationally simulate and experimentally measure. This difficulty in experimentally measuring the turbulent flux is due to the requirement that the concentration and three-component velocity data needs to be measured simultaneously.

Solving equation 1 in a simulation requires a solution for the turbulent flux term ($-\overline{cu_j}$), either through an accurate simulation or a model. When carrying out either Reynolds averaged Navier Stokes or large eddy simulations modelling this term is necessary. However, in direct numerical simulations or experimental studies, this term is accurately simulated.

2.3 Experimental Urban Cases

Experimentally measuring pollutant dispersion can be done through several methods, both intrusive and non-intrusive. In wind tunnels, the most common methods are to use a fast flame ionisation detector (FFID) (Carpentieri *et al.*, 2012) or photo-ionisation detector (PID) (Talluru *et al.*, 2018). These measurement techniques acquire concentration data at a single location at the head of a probe. Doing experiments in a water flume allows for the use of the planar laser induced fluorescence (PLIF) technique. This technique is a non-intrusive technique that quantitatively measures the fluorescence response of a dye in planar slices and calibrates this response to known dye concentration values.

There is a very limited amount of existing experimental data that includes both concentration and velocity measurements over realistic city models. The majority of existing experimental studies use either idealized urban roughness or fully randomized roughness (Fuka *et al.*, 2018). While idealized roughness can prove somewhat representative in highly ordered cities, such as Barcelona; most cities are built in a pseudo random form with neighbourhood scale order. Out of the existing aerodynamic studies into realistic city models, most are carried out in wind tunnels, in which acquiring full fields of concentration data is much more difficult than it is in water (Nironi *et al.*, 2015; Lim *et al.*, 2022). This means that most existing concentration data over realistic cities was taken using point measurement techniques; however, these methods have limitations when attempting to resolve highly heterogeneous roughness of the sort that is typical in realistic cities.

It has been shown that urban roughness increases the effective friction coefficient with increasing randomness in building element height (Xie *et al.*, 2008). It has also been shown that uniform roughness aligned with the flow has a lower friction coefficient than an equivalent patch of randomised roughness (Vanderwel & Ganapathisubramani, 2019). Urban landscapes fall somewhere in-between these two cases, and where they land is highly dependent on the wind direction at the time. Using these so called "idealised" cases to attempt to predict the behaviour of an urban flow field is clearly a complex task.

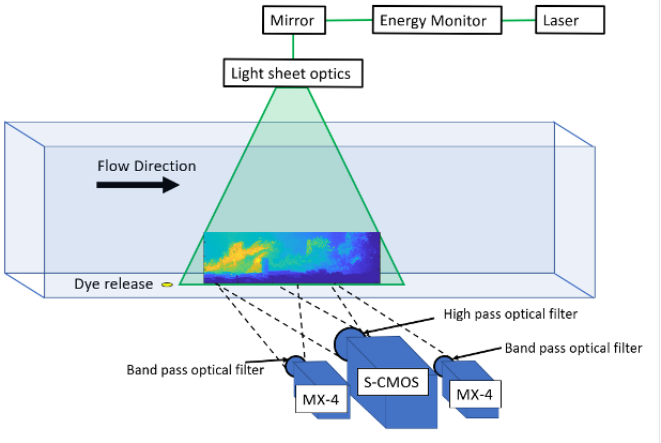

Figure 1. A diagram of the experimental setup used during acquisition of streamwise planar PIV-PLIF. This was carried out in the University of Southampton's recirculating water tunnel. The dye used for concentration measurements is visible under the laser sheet in this figure.

Figure 2. An image of the experimental setup used in this experiment series. In this image the upstream roughness elements are visible, followed by the 3D printed city model.

Measuring the flow over one particular city, and its effect on a pollutant plume is specific and non-generalisable. However, if the relationship between the idealised cases and realistic cases is ever to be understood then the first step is to measure the idealised cases, and the second step is to measure a realistic case and draw appropriate conclusions from this dataset about where similarities lie.

3 Methodology

3.1 Experimental Setup

Experimental measurements were made in the University of Southampton's Recirculating Water Tunnel (see figures 1 and 2). The city model is submerged in the water tunnel during the experimental campaign. This model was created to represent 1 km^2 of Southampton's city centre and the full to model scale is 1000:1. In this model, both terrain elevation and building height are represented, and the flow direction corresponds to the predominant wind direction of an onshore south-south-westerly. The section of the city chosen for measurements was selected to represent a pollutant release at the city port. This allowed the upstream edge of the model to be at sea level and not cause a step height change for the incoming flow.

The incoming flow was conditioned to have a boundary

layer depth of approximately 300 *mm* and a free-stream flow velocity of 0.6 m/s. Using the maximum building height of 45 *mm* as the length-scale, the Reynolds number was 27,000. Using the mean building height across the central section of the model of 20 *mm* gives a Reynolds number of 12,000. All data in this paper has been made dimensionless using a characteristic building height of $H = 20$ *mm*.

In order to experimentally simulate an onshore pollutant plume from the docks, a scalar source was introduced 50 *mm* upstream of the model. The scalar used was Rhodamine 6G fluorescent dye, which was illuminated using a Nd-YAG laser with an emission wavelength of 532 *nm*. This scalar was introduced with a low enough velocity that it did not measurably affect the velocity field, and was introduced at ground level through the use of a non-intrusive tube underneath the experimental setup.

This experimental setup was used so that both particle image velocimetry and planar laser induced fluorescence data could be acquired simultaneously with the one laser sheet to measure maps of flow velocity and concentration. PLIF data was post processed using custom Matlab code, while PIV data was processed using LaVision's Davis 10.2 software and then further post processed in Matlab.

Planar laser induced fluorescence works through the use of a camera with a long pass filter at the wavelength of the laser. This allows only the fluorescent response of the dye to be measured due to the emission being at a higher wavelength than the absorption (Vanderwel & Tavoularis, 2014). This fluorescent response can then be calibrated using the fluorescent responses of known dye concentrations. The result of this is a camera image in which each pixel corresponds to a local dye concentration within the laser sheet. When used with particle image velocimetry this allows both the velocity and concentration fields to be measured simultaneously. This enables the turbulent and advective components of concentration flux to be calculated across a laser sheet. In total, 14 measurements in the stream-wise vertical plane at 7 spanwise locations were captured, as well as 2 wall-normal orientations presented in figure 3. This many planes were required as the plume spread significantly as it progressed downstream, and this further highlights the effectiveness of using PIV-PLIF to capture full fields of data.

The convention used in this paper is to define downstream distance as x, cross-stream distance as y, and vertical distance as z. The scalar release location is chosen as the origin.

4 Results

4.1 Streamwise-vertical measurements

The mean velocity profiles over the city model are presented in figure 4 and appear relatively uniform regardless of location, with the exception of those in line with the tallest building. These profiles are well converged at a height of 240 *mm* or 12 H. This is still within the boundary layer depth of 300 *mm* (15H). The profiles in line with the tallest building along $y/H = -5$ (and shown in red in the figure) show that this row has a larger deficit than the rest of the measured area due to the local influence of the building.

Figure 5 shows an example of the PLIF concentration fields used to calculate the plume height. This is displayed on a log scale and the influence of the tall building on the region behind it is visible.

Figure 6 presents a map of the upper limit of the plume as defined as the isocontour of 0.002 percent of the source concentration. This plot was generated through the use of the

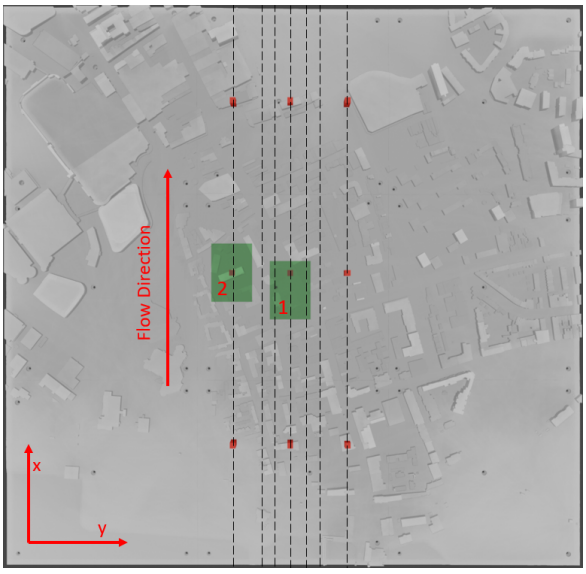

Figure 3. The 3D computational model that was used to generate the experimental 3D print. Dashed lines indicate the planes of the stream-wise vertical measurements. Green areas indicate the field of view of the wall-parallel measurements. Locations that the vertical profiles in figure 4 were extracted are represented as nine red dots.

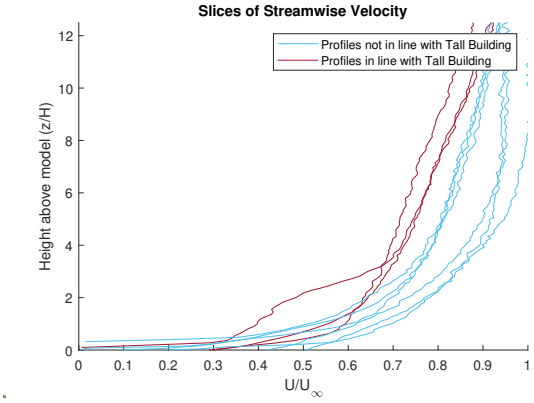

Figure 4. Vertical profiles of the streamwise velocity U/U_∞, extracted at locations shown in figure 3. The profiles in line with the tall building are shown in dark red, all others are shown in light blue. These are the left column of red dots on figure 4.

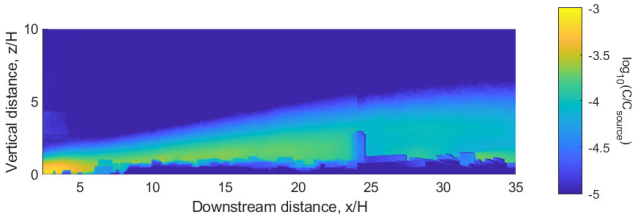

Figure 5. An example concentration field as measured using PLIF. This concentration field was extracted at $y/H = -5$, which is in line with the tallest building in the flow.

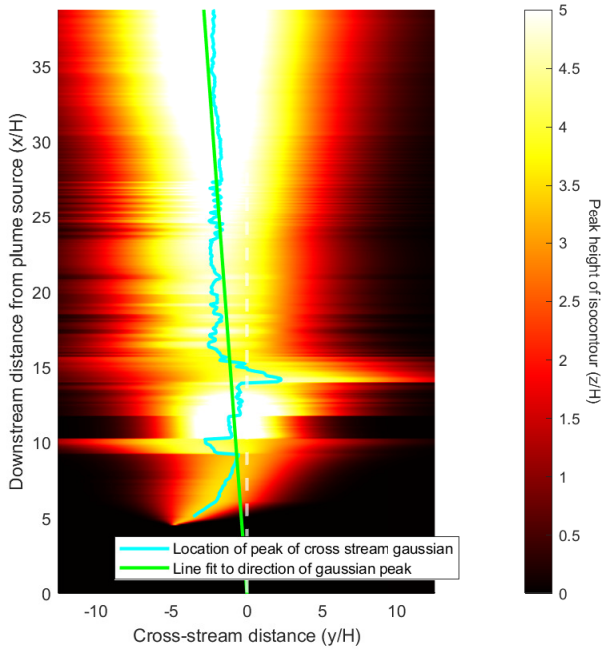

Figure 6. A map of the upper limit of the plume as defined as the isocontour of 0.002 percent of the source concentration. The displacement of the centre of the mean plume is shown in blue. The best-fit line in green shows the centre follows a mean direction of 4.2 degrees to the left of the mean flow direction.

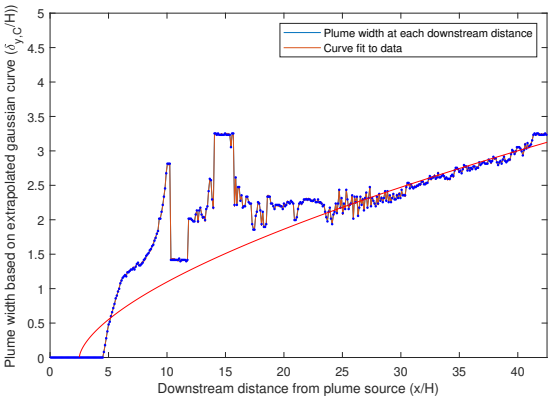

Figure 7. Plume half width against increasing downstream distance from the scalar source, this is defined using the half-max. This curve follows equation 2 and is only fit to data beyond $x/H = 20$.

seven streamwise-vertical slices. The isocontour heights were then extrapolated and interpolated in the cross-stream direction between the seven points assuming a Gaussian. This avoided any assumption of the streamwise development but did result in cross-stream bands in the image. Using the peaks of the plume height, it was calculated that the plume deflects from the mean flow direction by 4.2 degrees. We expect this is due to the mean street canyon orientation also being aligned towards the left side of the model.

Modelling this plume as a Gaussian allows the plume width $\delta_{y,C}$ to be defined as the halfwidth at halfmax, which is plotted in figure 7 as a funciton of downstream distance. The

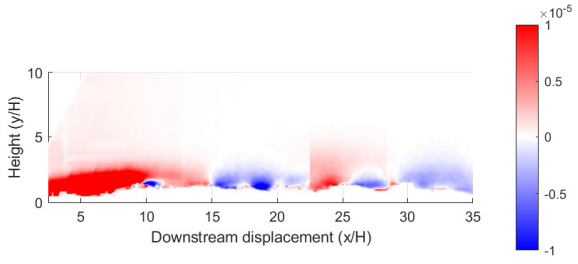

Figure 8. The vertical advective scalar flux ($\frac{CV}{C_s U_\infty}$) measured along the centreline of the city model.

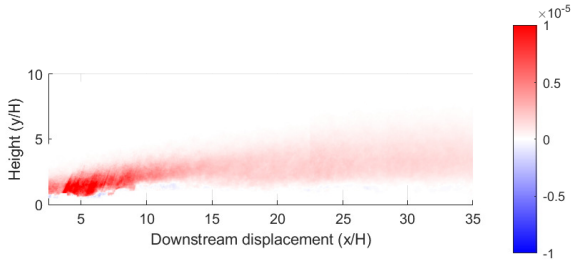

Figure 9. The vertical turbulent scalar flux ($\frac{\overline{c'v'}}{C_s U_\infty}$) measured along the centreline of the city model.

rate of spread can then be determined through the fitting of a power law curve to this dataset resulting in the function

$$\delta_{y,C}/H = 0.31\left(\frac{x-2.5}{H}\right)^{0.63}, \qquad (2)$$

following the form used by Lim & Vanderwel (2023) in which a virtual origin is used to aid in curve fitting. This curve fit was only calculated using data past $x/H = 20$ as we wouldn't expect a self-similar solution in the near field to the source. There is significant noise in the plume width and this is due to individual buildings affecting the plume locally. Particularly before $x/H = 20$, the change in plume width is believed to be due to local building effects.

It is possible that downstream of $x/H = 20$, the plume width growth slowing is in part due to the plume being funneled back towards the centre by the tall building to its left. It appears that within the far field, the assumption that the city acts as uniform roughness is generally accurate with respect to the lateral dispersion of the plume, but not its direction.

The vertical advective and turbulent fluxes are displayed in figures 8 and 9 respectively. We focus on the vertical fluxes as these are the most relevant for weather and pollution modelling. This data is taken from the centre plane of the flow and both are displayed on the same colourmap to allow for direct comparison. The turbulent flux field has a constant upwards direction at nearly all points in the flow, as is shown by the predominant red colour visible in figure 9. The sign of the advective flux field varies across the city model. As the scalar field has a constant positive sign, this is reflecting the varying sign of the vertical velocity component. This is most visible at $x/H = 22.5$ in figure 8 where the sign change happens close to a camera stitch line. It is noteworthy that both components of vertical transport are of similar average magnitudes.

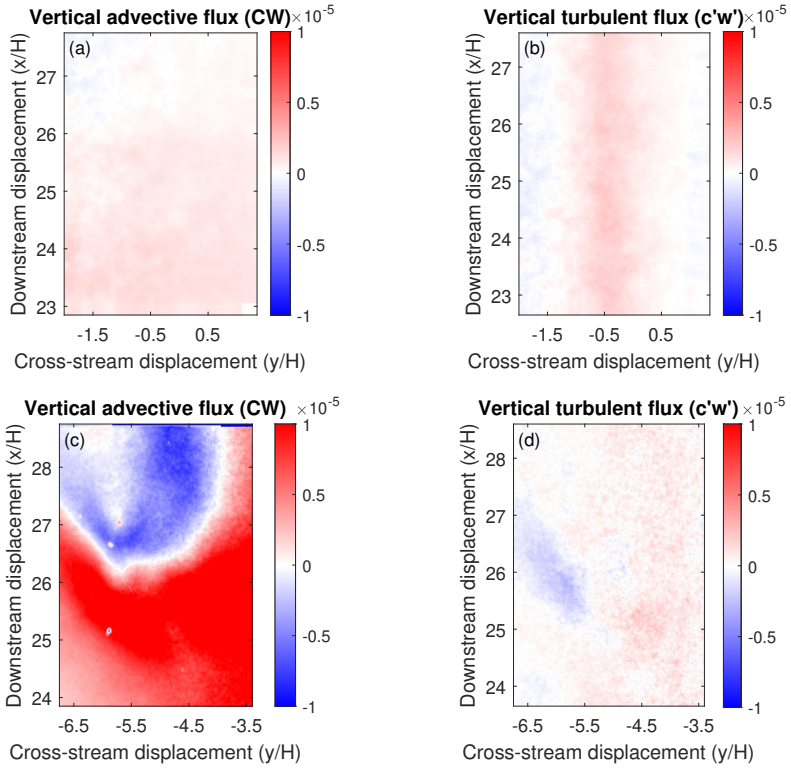

Figure 10. The vertical turbulent and advective flux fields above the centreline and tallest building of the city model, as marked in figure 3. Graphs (a) and (b) were extracted at position 1 in figure 3, graphs (c) and (d) were extracted at position 2. These slices were extracted at 3H (60mm) above the tunnel floor.

4.2 Wall-parallel measurements

Vertical turbulent and advective flux fields as measured in wall parallel slices at a height of 3H (60 *mm*) above the surface, are displayed in figure 10. Again these are displayed on the same colourmap as each other for direct comparison. These slices show that above the tallest buildings, the advective flux is uniformly positive in sign, with low variation across this city section. The turbulent flux is slightly higher along the centreline of the plume; however, the turbulent flux follows a less intuitive pattern than the advective flux's uniform distribution. Instead, the turbulent flux varies little with downstream distance, but shifts sign to negative off the centreline to either side.

Figure 10b also shows a slight displacement to the left of the centreline in the peak of the vertical turbulent flux. This effect is not visible in the vertical advective flux (figure 10a), but it agrees with the direction the plume has been shown to be displaced in figure 6.

The vertical turbulent and advective fluxes are of a similar order of magnitude across most of the model in both the stream-wise and wall parallel slices. The vertical turbulent flux always stays within the limits of the colourmap used in figures 8, 9, and 10. Mostly the advective flux also stays within this range; however, in locations with a particularly high mean vertical velocity, such as before the tallest building, the advective flux surpasses the turbulent flux by a large degree (figures 10c, 10d).

5 Discussion

We can identify 3 separate physical characteristics that influence the fluid flow and the pollutant plume dispersion over the city model. These are: (1) a highly rough surface increasing mixing and turbulence; (2) the neighbourhood-scale structures of street canyons creating large scale order; and (3) unusually large buildings creating large chaotic regions. This is suggested as an effective way to understand the effect of the pseudo-order present in urban landscapes.

The increased mixing from the roughness of the realistic city structure is shown in figure 7 by the rate at which the lateral plume width is growing over the model. This rate of growth of plume width implies high cross-stream scalar transport. Figure 9 shows that the vertical turbulent transport is also high, even relative to the advective transport displayed in figure 8.

The neighbourhood scale order in this particular urban case is present as an overall mean direction of the street canyons. These are mostly oriented either North-South, or East-West. With the incoming flow direction of South-South-West, the important street canyon is the North-South facing one. Figure 6 shows the deflection of 4.2 degrees in the scalar plume along the model that is hypothesised to be created by the street canyon orientation.

The particularly tall building along the left of the measurement area creates data that is anomalous to the two previously mentioned characteristics. The velocity fields in line with it (at $y/H = -5$) deviate from the general velocity fields above the city and show a persisting deficit due to the local effect of the building. The effect this building has on the concentration field is also noticeable and far reaching. It creates a lo-

cal zone in its wake of low concentration but pushes the upper edge of the plume higher than above the rest of the model. This agrees with what is expected from previous studies into scalar plumes near high aspect ratio buildings (Lim *et al.*, 2022).

6 Conclusion

This study has shown that across most areas of an urban flow, the magnitude of the vertical turbulent flux is very similar to the magnitude of the vertical advective flux. The vertical turbulent and advective fluxes also share no correlation in sign or strength, making the prediction of one using the other impossible. This demonstrates the difficulty in modelling the turbulent fluxes accurately, while also showing the importance of this modelling to simulating accurate results of scalar dispersion.

This study is one of very few to measure full fields of simultaneous concentration and velocity data over a realistic city model. By extension it is also one of the first measure full fields of the vertical turbulent flux for a realistic urban case.

The mean concentration data and plume shape indicate that the buildings are strongly influencing the shape of the plume away from what you would expect over regular or random roughness; this being a Gaussian plume following the mean flow direction. Instead, the plume still seems mostly Gaussian, but is diverted from its expected direction. The current hypothesis is that the plume is being influenced to follow the mean street canyon direction of the large street canyons. The mean velocity field reveals that the tallest building also has a very strong and widespread influence on the flow field over the city.

The conclusion that can be drawn from these measurements is that in most areas the city is acting as uniform roughness increasing the general turbulent mixing. The key exceptions to this rule are the neighbourhood scale order that is created due to street canyon alignment and the few particularly large buildings. On the 3D model, examples of these are located in regions 1 and 2 of figure 3 respectively. These urban features have a less predictable and stronger effect on the flow and the scalar plume, with their influence acting over a large local area.

Acknowledgements

We gratefully acknowledge funding from Christina Vanderwel's UKRI Future Leaders Fellowship (MR/S015566/1)

REFERENCES

Bermous, I. & Steinle, P. 2015 Efficient performance of the met office unified model v8.2 on intel xeon partially used nodes. *Geoscientific Model Development* **8**, 769–779.

Carpentieri, M., Hayden, P. & Robins, A. G. 2012 Wind tunnel measurements of pollutant turbulent fluxes in urban intersections. *Atmospheric Environment* **46**, 669–674.

City of London 2022 City of London, Micro climate Guidelines. `https://www.cityoflondon.gov.uk/services/planning/microclimate-guidelines`.

Dziubanek, G., Spychała, A., Marchwińska-Wyrwał, E., Rusin, M., Hajok, I., Ćwieląg-Drabek, M. & Piekut, A. 2017 Long-term exposure to urban air pollution and the relationship with life expectancy in cohort of 3.5 million people in Silesia. *Science of the Total Environment* **580**, 1–8.

Fuka, V., Xie, Z. T., Castro, I. P., Hayden, P., Carpentieri, M. & Robins, A. G. 2018 Scalar Fluxes Near a Tall Building in an Aligned Array of Rectangular Buildings. *Boundary-Layer Meteorology* **167** (1), 53–76.

Lim, H. D., Hertwig, D., Grylls, T., Gough, H., Reeuwijk, M. V., Grimmond, S. & Vanderwel, C. 2022 Pollutant dispersion by tall buildings: laboratory experiments and large-eddy simulation. *Experiments in Fluids* **63**.

Lim, H. D. & Vanderwel, Christina 2023 Turbulent dispersion of a passive scalar in a smooth-wall turbulent boundary layer. *Journal of Fluid Mechanics* **969**.

Met Office 2016 Our Supercomputer for Climate and Weather Dorecasting. `https://www.metoffice.gov.uk/about-us/who-we-are/innovation/supercomputer#:~:text=At%20the%20time%20of%20installation,dedicated%20to%20weather%20and%20climate.`

Met Office 2022 The Cray XC40 supercomputing system. `https://www.metoffice.gov.uk/about-us/what/technology/supercomputer`.

Nironi, Chiara, Salizzoni, Pietro, Marro, Massimo, Mejean, Patrick, Grosjean, Nathalie & Soulhac, Lionel 2015 Dispersion of a Passive Scalar Fluctuating Plume in a Turbulent Boundary Layer. Part I: Velocity and Concentration Measurements. *Boundary-Layer Meteorology* **156** (3), 415–446.

Talluru, K. M., Philip, J. & Chauhan, K. A. 2018 Local transport of passive scalar released from a point source in a turbulent boundary layer. *Journal of Fluid Mechanics* **846**, 292–317.

United Nations Department of Economic and Social Affairs 2018 68% of the world population projected to live in urban areas by 2050, says UN. `https://www.un.org/development/desa/en/news/population/2018-revision-of-world-urbanization-prospects.html`.

Vanderwel, C. & Ganapathisubramani, B. 2019 Turbulent Boundary Layers Over Multiscale Rough Patches. *Boundary-Layer Meteorology* **172** (1), 1–16.

Vanderwel, C. & Tavoularis, S. 2014 Measurements of turbulent diffusion in uniformly sheared flow. *Journal of Fluid Mechanics* **754**, 488–514.

Williams, M. & Barrowcliffe, R. 2011 Review of air quality modelling in DEFRA a report by the air quality modelling review steering group.

Xie, Z. T., Coceal, O. & Castro, I. P. 2008 Large-Eddy simulation of flows over random urban-like obstacles. *Boundary-Layer Meteorology* **129** (1), 1–23.